Oral exposure to zinc oxide nanoparticles induced oxidative damage, inflammation and genotoxicity in rat's lung

Howaida Nounou [1, 2], Hala Attia [3, 4], Manal Shalaby [2, 5], Maha Arafah [6]

[1.] Department of Medical Biochemistry, Faculty of Medicine, Alexandria University, Alexandria 21111, Egypt. Email: drhan2008@yahoo.com
[2.] Department of Biochemistry, College of Science, King Saud University, Riyadh, 11421
[3.] Department of Pharmacology and Toxicology, College of Pharmacy, King Saud University, Riyadh 11495, KSA.
[4.] Department of Biochemistry, Faculty of Pharmacy, Mansoura University, Mansoura 35516, Egypt.
[5.] Department of Biomedical technology, Institute of science biotechnology, City of scientific research and biotechnology. Alexandria 21111, Egypt. [6.] Department of Pathology, College of Medicine, King Saud University, Riyadh 11495

Abstract: This study aimed to investigate the toxicity of oral ZnONPs on the rat's lung. Rats were divided into four groups each of ten rats. Groups I and II were treated orally with 40 and 100 mg/kg ZnONPs for 24 hrs. Groups III and IV received daily 40 and 100 mg/kg ZnONPs orally for 1 week. Ten untreated rats were used as control. Oral administration of ZnONPs induced eosinophilia and lymphocytes infiltration in the lungs in the four tested groups that peaked at 100 mg/kg/day for 1 week. Lipid peroxidation was significantly higher, while levels of reduced glutathione and catalase activity were lower in all ZnONPs-treated groups. Nitrite concentrations increased significantly in rat's lung treated with 100 mg/kg for 24 hrs and in those treated with 40 and 100 mg/kg daily for 1 week. Levels of lung TNF-α were significantly higher after 24 hrs at high dose and after 1 week at both low and high doses. Interleukin-1β and pentraxin-3 levels were significantly increased at 1 week only at both low and high doses. There were lower levels of paraoxonase-1 and increased DNA damage in the four studied groups. Oral administration of ZnONPs induced lung injury possibly through oxidative stress, inflammatory response and DNA damage.

[Nounou H, Attia H, Shalaby M, Arafah M. **Oral exposure to zinc oxide nanoparticles induced oxidative damage, inflammation and genotoxicity in rat's lung**. *Life Sci J* 2013;10(1):1969-1979] (ISSN:1097-8135). http://www.lifesciencesite.com. 282

Keywords: ZnONPs; oxidative stress markers; inflammatory markers; DNA damage; lungs

1. Introduction

Nanoparticles (NPs) have unique and novel properties that lead to a diverse array of products with applications in diagnosis, drug delivery, food industry, paints, electronics, environmental cleanup, cosmetics and sunscreens **(Nohynek et al., 2007, Nel et al., 2009)**. Due to this expanding use of NPs and rapid growth in nanotechnology, the potential for human exposure has increased tremendously **(Roco, 2007).** It is necessary to assess the potential toxicity of engineered NPs to avoid their adverse effects on human health before widespread industrial application.

Zinc oxide nanoparticles (ZnONPs) are one of the most widely used engineered nanoparticles in consumer products. They are utilized in many commercial products including cosmetics, paints, textiles, and personal hygiene products. ZnONPs are highly effective in protection against ultraviolet A and B radiation; therefore, they are important ingredients of sunscreens and moisturizers **(Nohynek et al., 2007).** In addition, ZnONPs are being used in the food industry as additives and in packaging due to their antimicrobial properties **(Jin et al., 2009).** They also have potential use as fungicides in agriculture **(He et al., 2011)** and as anticancer in medical applications **(Rasmussen et al., 2010).** The increased production and use of ZnONPs enhances the probability of occupational and environmental exposure.

Experimental work done on cell cultures of colon cells compared the effects of ZnONPs to ZnO sold as a conventional powder. That experimental work found that the nanoparticles were twice as toxic to the cells as the larger particles **(Oberdörster et al., 2005).** The commonly proposed pathogenic mechanisms initiated by NPs are dominated by inflammation-driven effects; including fibrosis, oxidative stress, and DNA damage **(Nel et al., 2009, Lu et al., 2009).**

Most of toxicity studies of ZnONPs have mainly performed using cell lines. Exposure of human skin epithelial cells, for example, to ZnONPs produced severe cytotoxicity accompanied by oxidative stress and genotoxicity **(Kroll et al., 2009)**. While the in vitro assays have some limitations **(Sharma et al., 2009**), the in vivo systems involving; the complex cell–cell and cell–matrix interactions as

well as the diversity of cell types and hormonal effects are not present in cultured cells.

Few studies have been reported concerning the in vivo toxicity of ZnONPs although intratracheal instillation of ZnONPs in Sprague-Dawley rats induced cytotoxicity and severe inflammation after instillation **(Sayes et al., 2007, Cho et al., 2011).** Keeping in view the fact that ZnONPs can be ingested directly when used in food, food packaging, drug delivery and cosmetics, oral exposure and uptake through the gastrointestinal route needs to be considered. Workers involved in the synthesis of ZnONPs can be exposed by unintentional hand-to-mouth transfer of nanomaterials. When discharged accidentally into the environment, these nanoparticles may enter the human body through the food chain. Nanoparticles could be then translocated from the lumen of the intestinal tract and blood into different organs.

Previous experiments have revealed liver, kidney and spleen as the target organs for engineered nanoparticles after uptake by the gastrointestinal tract **(Wang et al., 2007).** However, a previous study had reported that, when 50 mg/kg and 300 mg/kg ZnO nanoparticle doses were administered orally by the gavage tube, elevated zinc levels were observed in the liver, lung, and kidney in 6–24 hours. This was explained by the ionization properties of ZnO nanoparticles following oral administration **(Baek et al., 2012).** Most studies on the toxicity of ZnONPs particles in mammals were focused on the pulmonary impact of inhaled ZnONPs nanoparticles or dermal exposure, but most available work has been undertaken on the impacts of oral exposure of these nanoparticles on the GIT and not on the lung. The present study was undertaken to investigate the oral toxicity of ZnONPs in lungs only and the mechanisms of toxicity involved. For this, we exposed rats to ZnONPs via the oral route and the toxic effects of nanoparticles on lung tissue were investigated. Oxidative tissue damage, inflammatory responses, genotoxic effects by comet assay, DNA fragmentation and organ damage by histopathology were investigated.

2. Material and Methods

Chemicals and reagents:

ZnONPs (<100 nm, surface area 15-25 m2/g, purity >99%, Cat. No. 544906) were obtained from Sigma-Aldrich (St Louis, Missouri, USA). Low melting point agarose (LMA), normal melting point agarose (NMA), ethidium bromide, thiobarbituric acid, Ellman's reagent (5, 5'-dithiobis-(2-nitrobenzoic acid, DTNB), sulfanilamide, N-(1-naphthyl) ethylenediamine dihydrochloride, were purchased from Sigma-Aldrich chemical Co. (St Louis, Missouri, USA). Kits for TNF-α and IL-1β were Quantikine Immunoassay kits (R&D Systems, Inc, Minnea- polis, USA), Pentraxin-3 kit was from CUSABIO BIOTECH Co., Ltd. (Wuhan, China) and paroxonase-1 kit was purchased from Life Science Co. (Florida, USA). All other chemicals used in this study were of high analytical grade.

Experimental animals and treatment:

The experimental procedures were carried out according to the National Institute of Health Guidelines for Animal Care and approved by the local Ethics Committee, IRB NO: 00007555. Adult male Wistar albino rats weighing 150-200 g were obtained from Animal Care Centre, College of Pharmacy, King Saud University, Riyadh, KSA. The animals were kept in a 12-hour light/dark cycle, at a temperature of 22°C ± 2°C with relative humidity 50% ± 20%. Animals were fed on standard food pellets and tap water ad libitum for the entire test period. The doses suggested in OECD TG 420 for investigating the oral toxicity of a new test chemicals are 5, 50, 300, 2000 and 5000 mg/kg. In case of ZnONPs and according to previous work **(Wang et al., 2007),** high doses showed extensive agglomeration which has suggested the need to study ZnONPs induced oral toxicity at low doses. While previous experiments had reported that, when 50 mg/kg and 300 mg/kg ZnO nanoparticle administered orally remarkable signs of toxicity had been observed in different organs including lungs **(Baek et al., 2012)** , we investigated toxicity of ZnONPs at concentrations 40 and 100 mg/kg. The rats were divided into 5 groups (10 rats in each group): control group, group I; low-dose one day group (40 mg/kg/24 hrs), group II; high-dose one day group (100 mg/kg/24 hrs), group III; low dose one week group (40 mg/kg/day for1 week), and group IV; high-dose one week group (100 mg/kg/day for 1 week). All animals were weighed at the beginning and end of each treatment. The ZnONPs suspension was given to rats by oral gavage tube according to body weight. The control groups received only the vehicle (distilled water) by oral gavage tube for 24 hrs and one week.

Particle characterization:

The morphology and size of ZnONPs was determined by transmission electron microscopy (TEM). The hydrodynamic size was determined using dynamic light scattering (DLS) in a Zetasizer Nano-ZS, Model ZEN3600 equipped with 4.0 mW, 633 nm laser (Malvern instruments Ltd., Malvern, UK).The surface zeta potential measurements were also performed with the Malvern Zetasizer Nano ZS. ZnONPs were suspended in Milli-Q water (filtered with 0.22 μm filter) at a concentration of 15 mg/ml and probe sonicated (Sonics & Material Inc., Newtown, CT, USA) at 30 W for 10 min (2.5 min on and 30 s off). For TEM a drop of ZnONPs solution (8

µg/ml in Milli-Q) was deposited on carbon-coated copper grids. The films on the TEM grids were allowed to dry prior to measurement **(Sharma et al., 2009).**

Preparation of ZnONPs:

ZnONPs were dissolved in distilled water in a concentration of 20 mg/ml for the dose of 40 mg/kg and in a concentration of 50 mg/ml for the dose of 100 mg/kg. The stock suspension was sonicated for 120 sec at a high energy level using a continuous mode to create a high grade of dispersion according to the protocol of **Bihari et al., (2008).**

Processing of lung tissue:

At specified time (24 hrs and one week); rats were anesthetized and sacrificed by decapitation. Lungs were isolated, immersed in normal saline and dissected into parts. One part of each lung was weighed and homogenized with phosphate buffered saline (PBS, pH 7.4) in an Ultra-Turrax homogenizer (IKA Labortechnik, Staufen, Germany). The homogenate was then centrifuged at 3,000 rpm for 10 min. at 4°C and supernatants were divided into aliquots and kept at -80° C for the subsequent assessment of oxidative stress and inflammatory markers, comet assay and DNA fragmentation. Small pieces of the other part of the lung were fixed in a 10% phosphate-buffered formalin solution thereafter; the organs were embedded in paraffin, stained with hematoxylin and eosin, and examined under light microscope.

Assessment of Oxidative Stress Markers

Assay of Lipid Peroxidation

Malondialdehyde (MDA, a product in the sequence of lipid peroxidation reactions) was quantified using thiobarbituric acid (TBA) assay as described by **Dubovskiy et al., (2008).** Briefly, 0.5 mL of 0.6 %TBA and 125 µL of 20% trichloroacetic acid (TCA) were mixed with 250 µL of lung homogenate. The mixture was heated for 30 min. in boiling water bath then cooled and centrifuged at 3000 rpm for 10 min. at 4°C. The absorbance of the developed pink colored chromogen was measured at 535 nm against reagent blank.

Assay of Reduced Glutathione (GSH)

GSH (the most important nonprotein sulphydryl antioxidant in the cell) was estimated using Ellman's reagent (5, 5'- dithiobis-2-nitrobenzoic acid; DTNB) according to the method described by **Moron et al., (1979)** with some modification. Briefly, a sample of lung homogenate was deproteinized by adding equal volume of 25% TCA and then centrifuged at 4°C at 3000 rpm for 10 minutes. 0.5 mL of supernatant was then added to 4.5 mL of Ellman's reagent and the produced yellow color was measured at 412 nm against reagent blank.

Assay of Catalase (CAT) Activity

CAT activity was estimated as the decomposition rate of hydrogen peroxide (H2O2) according to **Wang et al., (2001).** 500 µL 1% H2O2 in PBS was mixed with 5 µL of homogenate. The mixture was incubated at 28°C for 10 min and the rate of decomposition of H2O2 was measured at 240 nm.

Measurement of Nitrite (An Index of Nitric Oxide, NO) In Lung Tissues

Biologically produced NO is rapidly oxidized to nitrite and nitrate, thus, nitrite concentrations can reflect NO production, and may be measured colorimetrically using Griess reagent **(Kleinbongard et al., 2002).** 100 µL of tissue homogenate was added to 100 µL Griess reagent (1:1 mixture of 1% sulfanilamide in 2.5% orthophosphoric acid and 0.1% N-(1-naphthyl) ethylenediamine in distilled water). After 10 min of color development at room temperature, absorbance was measured at 540 nm.

Assessment of Inflammatory Markers:

Levels of tumor necrosis factor (TNF-α), interleukin-1β (IL-1β), pentraxin-3 (PTX-3) and paroxonase-1 (PON-1) in lung tissues were determined using ELISA technique according to the manufacturer's instructions.

Assessment of DNA damage:

Comet DNA Assay

The comet assay protocol was modified form previous report **(Hu et al., 2002)**. Lung was minced, suspended in 4mL, chilled homogenizing solution (pH 7.5) containing 0.075 M NaCl and 0.024 M Na2EDTA and then homogenized gently using a potter-Elvehjem homogenizer at 500 to 800 rpm in ice. To obtain nuclei, the homogenate was centrifuged at 700 X g for 10 min at 0°C and the precipitate was resuspended in chilled homogenizing buffer at 1 g organ weight/mL. 100 µL of lung homogenate was mixed with 600 µL of low-melting agarose (0.8% in PBS, Sigma, USA). 100 µL of this mixture was spread on slides pre-coated with 300 µL of 0.6% normal melting point agarose (NMP). After application of a third layer of 0.6 % NMP (300 µL), slides were immersed in ice-cold lysis buffer (0.045 M Tris-borate-EDTA (TBE) buffer, pH 8.4) for 1 hrs at 4°C. Slides were then removed from the lysing solution and placed for 20 min in a horizontal electrophoresis unit filled with an alkaline buffer (1 mM Na2 EDTA and 300 mM NaOH, pH 13) to allow the unwinding of DNA. After the unwinding of DNA, electrophoresis was carried out under standard conditions (25 V, 300 mA, distance between electrodes 30 cm) for 20 min. at room temperature in the same alkaline solution (pH 13). Electrophoresis at high pH results in structures resembling comets, as observed by fluorescence microscopy; the intensity of the comet tail relative to the head reflects the number of DNA breaks. The slides were then neutralized by adding 0.4 M Tris–

HCl buffer (pH 7.5), stained with ethidium bromide (20µg/ml, Sigma USA) at 4°C, covered and stored in sealed boxes at 4°C until analysis. All preparation steps were performed under dimmed light to prevent additional DNA damage by UV. Images of 100 randomly selected cells were analyzed for each sample. DNA fragment migration patterns was evaluated with Leitz Orthoplan epifluorescence microscope (magnification 250×) equipped with an excitation filter of 515–560 nm and a barrier filter of 590 nm. The microscope was connected through a camera to a computer-based image analysis system (Comet Assay IV software, Perspective Instruments). Comets were randomly captured at a constant depth of the gel, avoiding the edges of the gel, occasional dead cells, and superimposed comets. DNA damage was measured as tail length (TL = distance of DNA migration from the centre of the body of the nuclear core, tail intensity DNA (TI = % of DNA that migrated from the nuclear core to the tail) and tail moment. The tail moment (TMOM) was determined according to the formula:

TMOM =DNA in tail as a % of total DNA x tail length (TL).

Measurement of DNA fragmentation

The fragmented DNA was quantified using diphenylamine (DPA) reagent according to the method of **Burton (1956)** and modified by **Suenobu et al., (1999)**. Lung homogenate were lysed with 0.4 mL hypotonic lysis buffer (10 mmol/L Tris, 1 mmol/L EDTA, and 0.1% NP-40, pH 7.5) and centrifuged at 13000 g for 10 minutes to separate intact from fragmented chromatin. The supernatant containing fragmented DNA was placed in a separate Microfuge tube, and both pellet and supernatant were precipitated overnight at 4°C in 12.5% trichloroacetic acid. The precipitates were sedimented at 13000 g for 4 minutes. The DNA precipitates were hydrolyzed by heating to 90°C for 10 minutes in 5% trichloroacetic acid. For quantification of fragmented DNA, in brief, 0.16 mL of DPA reagent (0.15 g DPA, 0.15 mL H2SO4, and 0.05 mL acetaldehyde per 10 mL glacial acetic acid) was added to each tube, and the absorbance at 570 nm was measured after overnight color development. "Percent fragmentation" refers to the ratio of DNA in the supernatant ("fragmented") to the total DNA recovered in both supernatant and pellet ("fragmented plus intact").

Statistical analysis:

Results are expressed as mean ± SEM. Statistical comparisons between groups were performed using one way analysis of variance (ANOVA) followed by Tukey Krammer as post multiple test. Statistical analysis was performed using Graph pad Instat 3 software Inc, San Diego, CA, USA. Results were considered significant at $P<0.05$.

3. Results

Particle characterization:

The counted particles by TEM were 105 and no aggregation could be detected as shown in Figure

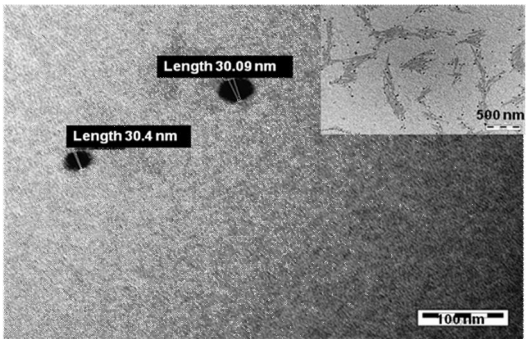

Figure 1, ZnONPs demonstrated a spheroid shape; the minimum size was 23 nm and the maximum was 34 nm. The mean size measured by the TEM was 30 nm with a standard error ± 1.12. The mean hydrodynamic diameter of the nanoparticle suspension in Milli-Q water as determined by the DLS measurement was 272 nm ± 8.75 (minimum diameter was 234 nm and the maximum was 386 nm). The surface zeta potential was – 41.2 ± 0.65 mV. Data are reported as mean ± SE.

Biochemical Measurements in Lung Tissues:

There was no difference between the results of the two control groups, so for simplicity the two control groups for 24 hrs and 1 week were combined in one control group.

Oxidative Stress Markers in Lung Tissues

A significant elevation of malondialdehyde (MDA; a marker of lipid peroxidation) in lung tissues was observed in all groups treated with ZnONPs at different doses (40 mg/kg and 100 mg/kg) and for different durations (24 hrs and 1 week) compared to the normal control group ($P < 0.01$, $P < 0.001$, respectively). As shown in Figure (2A), the level of MDA was significantly higher in the rats treated at 100 mg/ kg/day for1 week (group IV) compared to those treated at 40 and 100 mg for 24 hrs (groups I, II, $P < 0.001$) and to those treated at 40 mg/ kg/day for 1 week (group III, $P < 0.01$).

Reduced glutathione (GSH) levels were significantly lower in lung tissues in the four studied groups compared to the normal control group ($P < 0.05$, $P <0.001$), also there was a significant decrease in GSH levels in the rats treated daily with ZnONPs for 1 week at both low and high doses (40 and 100 mg/kg) (groups III, IV) compared with those treated for 24 hrs at a dose of 40 mg/kg (group I) ($P < 0.01$) Figure (2B).

Figure (2C) demonstrates that all the four studied groups, showed significant decrease in catalase (CAT) activity in lung homogenates compared to the normal control group ($P < 0.05$, $P < 0.01$, $P < 0.001$). As shown in Figure (2D), nitrite concentrations in lung tissues were increased in all groups, however the increase was highly significant in the rats treated at high dose (100mg/kg) for 24 hrs (group II), and in those treated at both low and high doses (40 and 100 mg/kg) for one week (groups III, IV) compared to the control group. The increase was time-dependent since nitrite concentrations in rats treated with ZnONPs 100mg/kg/day for 1 week (group IV) showed a significantly higher levels as compared to those treated with 40 and 100 mg/kg/24 hrs (groups I, II) while nitrite concentrations were significantly higher in rats treated with ZnONPs 40mg/kg/day for 1 week (group III) than group I treated with 40mg/kg/24 hrs.

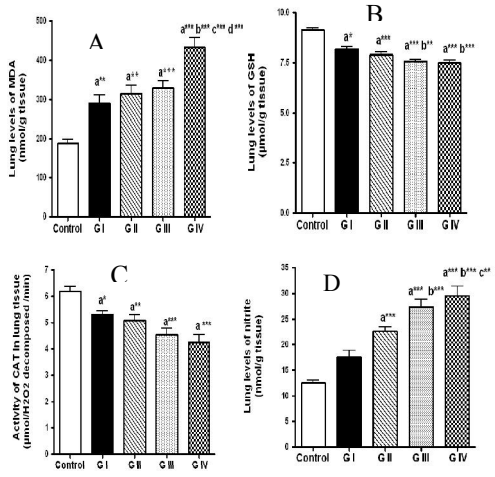

Figure 2, Levels of oxidative stress markers in lung tissues in the different studied groups. A: malondiladehyde (MDA); B: reduced glutathione (GSH); C: catalase activity (CAT) and D: nitrite (as index of NO). Data are expressed as mean ± SEM of 10 rats in each group. Control group, G I rats treated at 40 mg/kg/24 hrs and G II rats treated at 100 mg/kg/24 hrs, G III rats treated at 40 mg/kg/day for 1 week and G IV rats treated at 100 mg/kg /day for 1 week. a: significantly different from normal control rats; b: significantly different from group I (40 mg/kg/24 hrs); c: significantly different from group II (100 mg/kg/24 hrs); d: significantly different from group III (40 mg/kg/day for 1 week) *: P<0.05; **: P<0.01; ***: P<0.001

Pro-inflammatory and anti-inflammatory markers in lung tissues:

The concentrations of TNF-α, IL1-β and PTX-3 were significantly higher in ZnONPs- treated groups at 1 week either at the low dose (40 mg/kg/day for 1 week) or the high dose (100 mg/kg/day for 1 week) (groups III, IV) compared to the normal control group ($P < 0.001$) (Figure 3). TNF-α levels were significantly higher in the rats treated with ZnONPs at a high dose 100 mg/kg /24 hrs (group II) and in the groups treated at 40 and 100 mg/kg/day for 1 week (groups III, IV), compared to group I (40 mg/kg/24 hrs, $P < 0.001$) Figure (3A).

Oral treatment with ZnONPs produced significant increases in IL-1β and PTX-3 as two inflammatory biochemical parameters at 1 week in group III (40mg/kg/day for 1 week) and group IV (100 mg/kg/day for 1 week) compared to control whilst, at 24 hrs in group I (40 mg/kg) and group II (100 mg/kg) there were no significant changes compared to control (Figures 3B, 3C). IL-1 β and PTX-3 concentrations were elevated in group IV that was treated at high dose for one week (100 mg/kg) compared to the concentrations observed in groups treated for 24 hrs either at low (40 mg/ kg) or high (100 mg/ kg) doses (groups I, II).

Activity of PON-1 which is antioxidant and anti- inflammatory was significantly lower in all the four studied groups compared with normal control group ($P < 0.01$, $P < 0.001$). There was a significantly decreased activity in group II (100 mg/kg/24 hrs) as compared to group I (40 mg/kg/24 hrs). Groups that were treated daily for 1 week (groups III 40mg/kg and IV 100mg/kg) showed highly significant reduction in PON-1 activity compared to those treated for 24 hrs (groups I 40mg/kg and II 100mg/kg) ($P < 0.001$). There was no significant difference in PON-1 activity in group IV that was treated at high dose 100 mg/kg/day for 1 week compared with those treated at low dose group III 40 mg/kg/day for 1 week (Figure 3D).

Assessment of DNA Damage:

Comet DNA assay in lung tissues

Comet DNA assay as a marker for DNA fragmentation was significantly increased in the four studied groups compared to the normal control group and was maximum in ZnONPs treated with 100 mg/kg/day for 1 week (group IV). Treatment daily for one week at both low and high doses 40 and 100 mg/kg (groups III, IV) showed increased DNA damage as compared to treatment for 24 hrs (groups I, II) (Figure 4 and Table 1 a, b). These results were ascertained with the % DNA migrated (TI) which shows same pattern of changes. Tail moment showed similar results however non significant increase was observed with group I (40 mg/kg/24 hrs) compared with normal control.

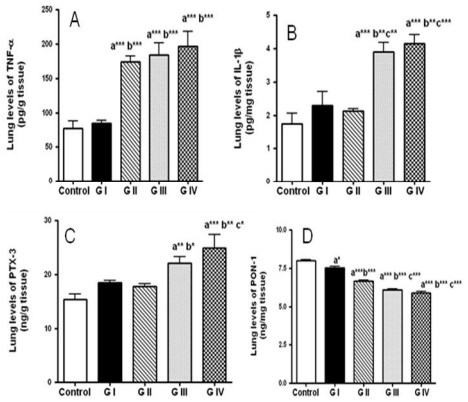

Figure 3, Levels of pro-inflammatory and anti-inflammatory markers in lung tissues A: Tumor necrosis factor- α (TNF-α); B: interleukin-1β (IL-1β); C: Pentraxin-3 (PTX-3) and D: Paroxonase-1(PON-1). Data are expressed as mean ± SEM of 10 rats in each group. Control group, G I rats treated at 40 mg/kg/24 hrs and GII rats treated at 100 mg/kg/24 hrs, G III rats treated at 40 mg/kg/day for 1 week and G IV rats treated at 100 mg/kg /day for 1 week. a: significantly different from normal control rats; b: significantly different from group I (40 mg/kg/24 hrs); c: significantly different from group II (100 mg/kg/24 hrs); *: P<0.05; **: P<0.01; ***: P<0.001.

Table 1 (a). Comet DNA assay in lung tissues

Group	Tailed DNA %	P value	Tail length (µm)	P value
Control	4.25 ± 0.31		2.51 ± 0.116	
G I	8.33 [a] ± 0.25	[a] *P<0.001*	3.91 [a] ± 0.12	[a]*P<0.001*
G II	11.17[a b] ± 0.33	[a,b]*P<0.001*	5.02[ab] ± 0.17	[a]*P<0.01* [b] *P<0.05*
G III	15.2 [a b c] ± 0.34	[a,b,c]*P<0.001*	7.95[abc]± 0.19	[a,b,c]*P<0.001*
G IV	20.33[abcd] ± 0.67	[a,b,c,d]*P<0.001*	11.37[abcd]± 0.38	[a,b,c,d]*P<0.001*

Table 1 (b). Comet DNA assay in lung tissues (Cont.)

Group	Tail intensity (TI)	P value	Tail moment	P value
Control	2.23 ± 0.085		5.36 ± 0.24	
G I	3.86 [a] ± 0.111	[a]*P<0.001*	15.31 ± 0.64	Ns
G II	4.63 [a] ± 0.2	[a]*P<0.001*	22.47 [a] ± 0.17	[a] *P<0. 01*
G III	6.42 [a b c] ± 0.2	[a,b,c]*P<0.001*	50.03[a,b,c] ± 1.46	[a,b,c] *P<0.001*
G IV	9.22[a b c d] ± 0.67	[a,b,c,d]*P<0.001*	108.2 [a b c d] ± 7.44	[a,b,c,d]*P<0.0 01*

Data are expressed as mean ± SEM; NS: not significant; a: significantly different from normal control rats. b: significantly different from group I (40 mg/kg/24 hrs); c: significantly different from group II (100 mg/kg/24 hrs); d: significantly different from group III (40 mg/kg/day for 1 week).

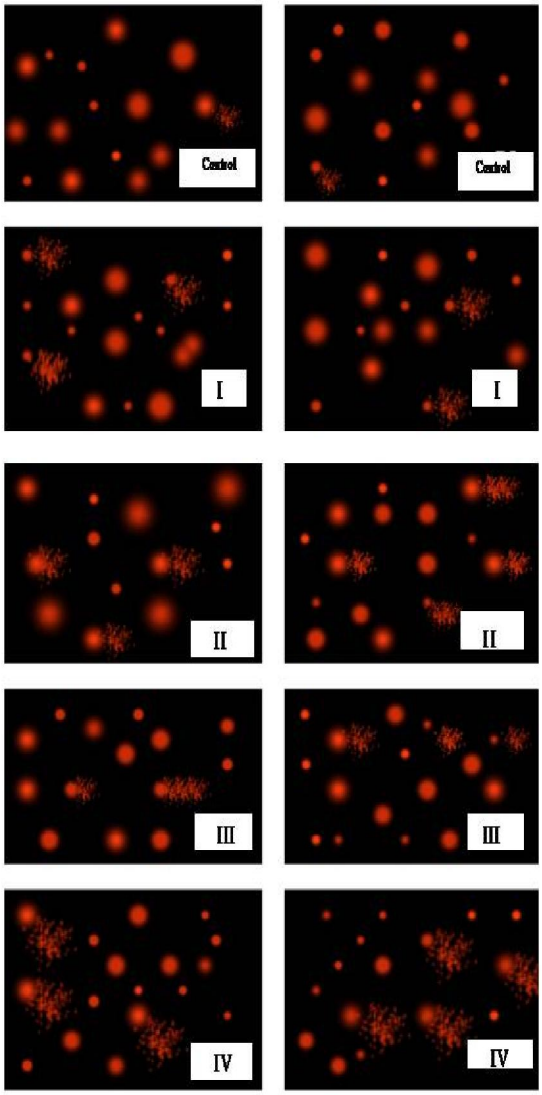

Figure 4, Comet DNA assay in lung tissues. Control group, G I rats treated at 40 mg/kg/24 hrs and GII rats treated at 100 mg/kg/24 hrs G III rats treated at 40 mg/kg/day for 1 week and G IV rats treated at 100 mg/kg/day for 1 week. Tail length as marker for DNA fragmentation has increased in the four studied groups compared to the normal control group and was maximum in G IV (100 mg/ kg/day for1 week).

DNA fragmentation in lung tissues and its correlations with PON-1

DNA fragmentation % was significantly higher (P< 0.001) in the four ZnONPs treated groups

compared to the normal control group as shown in Table 2 which confirm the DNA comet assay results. Data of at least six rats showed that, there were negative correlations between DNA fragmentation and PON-1 concentrations in all studied four groups which were significant in groups II, III and IV (G I, r = - 0.63, P=0.086; G II, r = - 0.751, P <0.05; G III, r = - 0.93, P <0.001 and G IV, r = - 0.882, P <0.001) (Figures 5, 6).

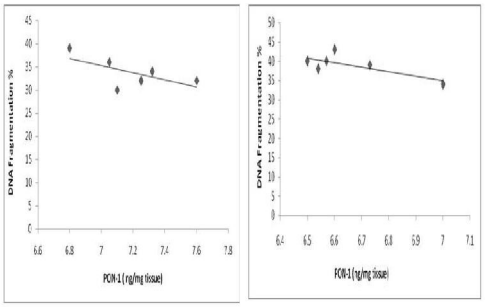

Figure 5, Negative correlation between DNA fragmentation and concentrations of PON-1 (ng/mg tissue) in lung in rats administered ZnONPs for 24 hrs (A): 40 mg/kg ZnONPs (G I, r = -0.638, P=0.086) and (B): 100 mg/kg (G II, r = - 0.751, P<0. 05).

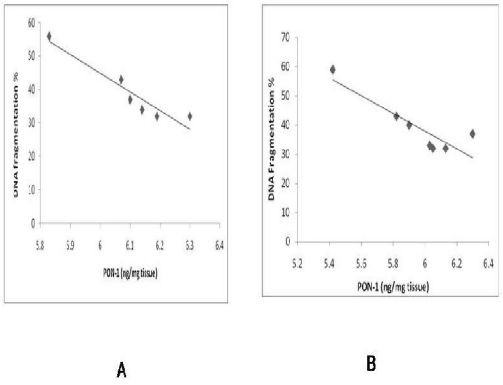

Figure 6, Significant negative correlation between DNA fragmentation and concentrations of PON-1 (ng/mg tissue) in lung tissues of rats administered ZnONPs daily for 1 week at (A): 40 mg/kg ZnONPs (G III, r = -0.93, P<0.01) and (B): 100 mg/kg (G IV, r = -0.882, P<0.01).

Table 2. DNA fragmentation in lung tissues.

Groups	DNA fragmentation (%)
Control	10.36 ±1.77
G I (40 mg/kg/24 hrs)	33.53 ^{a***} ± 1.34
G II (100 mg/kg/24 hrs)	38.65 ^{a***} ± 2.7
G III (40 mg/kg/day for 1 week)	36.9 ^{a***} ± 4.18
G IV(100 mg/kg/day for 1 week)	39.52 ^{a***} ± 3.633

Data are expressed as mean ± SEM of 10 rats in each group; a: significantly different from normal control rats ***: P<0.001.

Lung histopathology (H & E):

ZnONPs induced diverse pathological lung lesions when rats were treated with both low (40 mg/ kg) or high (100 mg/ kg) doses either for 24 hrs only or for 1 week. The representative pathological lesions could be classified as eosinophilic inflammation, lymphocytes and mast cells infiltration around arterioles, in the alveolar interstitium and hemorrhage. Number of eosinophils around arterioles and bronchioles and hemorrhage, were remarkably increased among all the studied groups and peaked at 1 week after oral treatment with ZnONPs 100mg/ kg (group IV). Furthermore, dense infiltration by lymphocytes and macrophages was observed after one week in groups III and IV (Figures 7, 8).

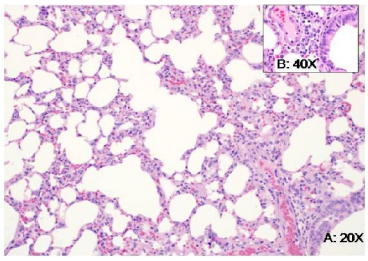

Figure 7, H& E stain of lung tissues in the control group. A few lymphocytes and other mononuclear cells in the interstitium and around the bronchioles in the control lung. H&E; A is 20X and B is 40X.

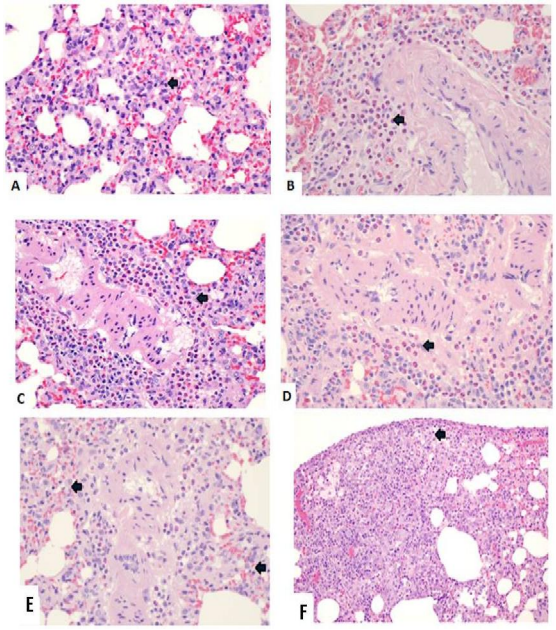

Figure 8, H& E stain of lung tissues in the studied groups. A: GI (40mg/kg/24 hrs): infiltration by mononuclear cell in the interstitium with hemorrhage. H&E 40X. B. G II (100 mg/kg/24 hrs): infiltration by

eosinophils and mast cells in the interstitium and around the arterioles associated with mild hemorrhage, H&E 40X. C: G III (40 mg/ kg/day for 1 week): infiltration by eosinophils and mononuclear cells in the interstitium and around arterioles with hemorrhage. H&E 40X. D: G IV (100 mg/kg/day for 1 week): Dense infiltration by eosinophils and other mononuclear cells around arterioles. H&E 40X. E& F: G IV (100 mg/ kg/day for 1 week): Dense infiltration by lymphocytes, eosinophils and other mononuclear cells in the interstitium (E) H&E. 40X and subpleural areas (F) with hemorrhage H&E 20X.

4. Discussions

The escalating uses of zinc oxide nanoparticles (ZnONPs) in coatings, paints, personal care products, food industry and medical applications increase the possibility of different organs exposure to ZnONPs. In the present study, oral administration of ZnONPs caused severe inflammatory lung injury, in groups treated with 40 and 100 mg/kg for either 24 hrs or one week, as observed with H&E staining showing eosinophilic inflammation, hemorrhage in addition to lymphocytes and mast cells infiltration. These results were similar to intratracheal instillation studies in which neutrophilic and eosinophilic inflammation was reported using ZnONPs (Sayes et al., 2007, Cho et al., 2011), indicating that pulmonary toxicity of ZnONPs is elicited not only by direct instillation or inhalation but extended to oral exposure.

One of the proposed mechanisms of ZnONPs-induced lung injury is the release of reactive oxygen species (ROS) with the subsequent oxidative stress. Oxidative damage of ZnONPs on lung tissues was indicated in our study by the higher levels of MDA; a product of lipid peroxidation, together with lower levels of GSH and CAT activity in lung tissues treated with ZnONPs compared to normal control. These effects were observed by both 40 and 100 mg/kg either at 24 hrs and one week. Decreased GSH levels with the duration of ZnONPs exposure (Figure 2B) indicated time-dependent elevation of oxidative stress in the lung. Significant increased levels of MDA in group IV (100 mg/kg/day for 1 week) compared to group III (40 mg/kg/day for 1 week) may reflect the dose dependent effect of ZnONPs toxicity (Figure 2A). Our results are consistent with previous studies suggesting that cytotoxcity of ZnONPs was mediated through ROS generation and oxidative stress (**Hackenberg et al., 2011, Huang et al., 2010).** Lipid peroxidation; the peroxidative breakdown of polyunsaturated fatty acids, leads to lung injury due to the effects on membrane function, inactivation of membrane-bound receptors and enzymes, and increased tissue permeability **(Rahman, 2005).** Several studies have suggested that GSH homeostasis may play a central role in the maintenance of the integrity of the lung airspace epithelial barrier. It has been shown that GSH depletion, as observed in our study by all groups treated with ZnONPs, sensitizes both alveolar and bronchial epithelial cells to the injurious effects of H2O2, resulting in an increased membrane permeability and activation of nuclear factor kB (NF-kB) leading to inflammation **(Rahman et al., 2001).** Under normal conditions, scavenging of H_2O_2 is catalyzed by catalase enzyme, which activity was significantly decreased in the present study by all the four studied groups treated with ZnONPs (Figure 2C).

Reactive nitrogen species, derivatives of nitric oxide (NO), have also been implicated in oxidative stress. In the present study, the levels of nitrite (a stable metabolite of NO) were markedly increased in the lung homogenate of rats treated with 100 mg/kg/24 hrs and in those treated with either 40 or 100 mg/kg/1 week (Figure 2D) reflecting increased NO production possibly through activation of NO synthase (NOS). Increased nitrite levels with the duration of treatment [levels in rats treated daily for 1 week at either low or high doses were significantly higher than levels in rats treated for 24 hrs] may indicate time-dependent effect of ZnONPs on lung injury. Neutrophils and macrophages are generally considered to be the most prodigious source of highly reactive oxidants in the lung **(Brigham, 1986).** It is postulated that ZnONPs may be capable of priming and/or activating neutrophils to generate ROS and to stimulate NOS to produce more NO in lung tissues.

Second possible mechanism of the toxic effect of ZnONPs on lung is the inflammatory response. Levels of lung TNF-α were significantly increased after 24 hrs at high dose (group II) and after one week of administration of ZnONPs at both low and high doses (groups III, IV). Oral treatment with ZnONPs produced significant increases in IL-1β at 1 week (groups III, IV) whilst at 24 hrs (groups I, II) there were no significant changes compared to control (Figure 3B). Collectively, these data may suggest the role of TNF-α in acute oral toxicity, while IL-1β was involved in long term inflammatory response, this may be because TNF-α represents an early phase mediator of inflammation **(Pereda et al., 2006).** It was revealed that nanoparticles are more potent in instigating the proinflammatory cytokine production by macrophages compared to bulk size ZnO **(Roy et al., 2011),** indicating that their small size may help in evading the macrophage response. Pulmonary inflammation in the current study may be also attributed to ZnONPs-induced ROS which has been implicated to enhance gene expression of pro-inflammatory mediators **(Kamata et al., 2005).** Likewise, lipid peroxidation products have also been shown to act as a signal for activation of transcription

factors and gene expression, leading to an inflammatory response **(Uchida et al., 1999)**. Direct or indirect oxidant stress to the airway epithelium and alveolar macrophages may also generate cytokines, such as TNF-α, which in turn can activate airway epithelial cells to induce proinflammatory genes **(Rahman, 2005).**

Pentraxin-3 (PTX-3) is a glycoprotein belonging to the pentraxin family of acute-phase proteins. It was originally described as a gene inducible by TNF-α in human fibroblasts and, soon after, it was also identified as being induced by IL-1β in endothelial cells **(Breviario et al., 1992).** Increased PTX-3 levels were found in the lung tissue in multiple models and their levels were strikingly correlated with the severity of lung injury **(Okutani et al., 2007).** This finding supports our results where PTX-3 levels in the lung tissues were significantly elevated compared to normal control only after administration of ZnONPs for one week either at 40 or 100 mg/kg, while non significant increase was observed with 24 hrs treatment at both low and high dose (Figure 3C). In our study severe inflammation and hemorrhage were clearly recorded in groups III and IV. Increased PTX-3 in groups III and IV could be explained by either the direct effect of cumulative doses of ZnONPs that may induce PTX-3 gene expression in the rat's lung or by the consequence of elevated IL-1β and TNF-α, such explanation is potentiated by cell culture studies in which treating lung cells with TNF-α or IL-1β induced a significant increase in PTX-3 gene expression and protein production **(Souza et al., 2002, Han et al., 2005).**

Paraoxonase-1(PON-1) is an antioxidant that has been suggested to play an important role in metabolizing and detoxifying lipid peroxides **(Harangi et al., 2004).** The results of our study showed lower activities of PON-1 in all the four studied groups compared to normal control (Figure 3D). As reported by **Feingold et al., (1998**) and **Kumon et al., (2003),** PON-1 was down-regulated by the administration of TNF-α and IL-1β, therefore, we suggest that the decrease in lung PON-1 activity in our study may be secondary to inflammatory response in ZnONPs-treated groups. We also can conclude that the reduction of PON-1 activity, may contribute to oxidative damage of ZnONPs in the lung tissues.

Although the genotoxic potential of ZnONPs has been reported **(Sharma et al., 2009, Wang et al., 2007, Hackenberg et al., 2011, Yang et al., 2009, Lin et al., 2009)**, however, there is a lack of information on oral ZnONPs-induced DNA damage. Our results showed DNA damage in all groups treated orally with ZnONPs compared to normal control as demonstrated by comet assay (Figure 4 and Tables 1a and 1b) and DNA fragmentation (Table 2). The longer DNA tail lengths represent higher percentages of DNA strand break. In our study, tail length and tail moment were significantly increased in the four studied groups compared to the normal control in both dose and time-dependent manner (Tables 1a and 1b). DNA damage may occur due to direct interaction of ZnONPs with the DNA after its nuclear uptake, or by intracellular ROS generation induced by ZnONPs **(Hackenberg et al., 2011).** Products of lipid peroxidation can interact with DNA causing genetic damage and disturbance of cell signaling **(Harangi et al., 2004)**. The PON-1, via hydrolyzing lipid peroxides, inhibits the development of further oxidative stress and thus, prevents the oxidative damage of DNA (Harangi et al., 2004). Accordingly, in the current study, the significantly reduced levels of PON-1 in ZnONPs-treated rats are postulated to play a crucial role in ZnONPs-induced DNA damage. This finding was further confirmed by the negative correlations found in our study between DNA fragmentation and PON-1 activity in all studied groups with significant correlation detected in groups II (100mg/kg/24 hrs) , III (40mg/kg/day for 1 week) and IV (100mg/kg/day for 1 week) (Figures 5 and 6). Our results are similar to those carried out on cell lines that reported oxidative DNA damage after exposure to ZnONPs **(Sharma et al., 2009, Hackenberg et al., 2011, Lin et al., 2009).** Ongoing DNA damage in groups III (40mg/kg/day for 1 week) and IV (100mg/kg/day for 1 week) could be attributed to the persisting presence of intracellular ZnONPs, which may even increase with time because of the release from endocytotic vesicles or continued cellular uptake. Effects of ZnONPs on the oxidative stress, antioxidants, selective inflammatory markers and DNA damage are summarized in the illustrated **figure 9.**

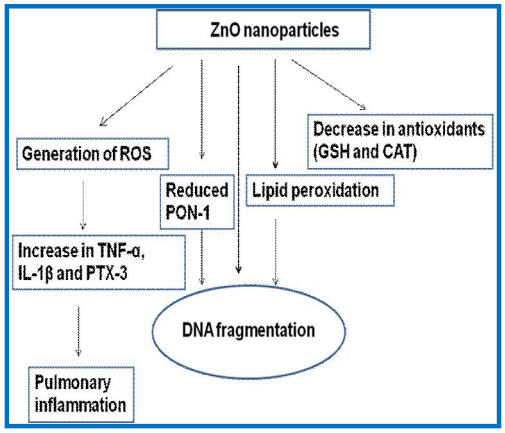

Figure 9, effects of ZnONPs on oxidative stress, antioxidant system, mediators of inflammation and DNA damage as suggested by the results of the present study.

Most studies focus on the toxic effect of ZnONPs on lung when administered through inhalation. Our result highlighted that the oral administration of ZnONPs also poses a unique and substantial hazard to the lungs via a multitude of mechanisms. ZnONPs induced oxidative damage as evidenced by the elevation of lipid peroxidation and the decline of the antioxidants; GSH, CAT and PON-1. In addition, they resulted in inflammatory response through release of TNF-α, IL-1β and PTX-3 as well as gentoxicity through DNA damage. These results emphasize the need for caution during the use and disposal of such manufactured nanomaterials to prevent unintended environmental impacts.

Acknowledgements:

The authors extend their appreciation to the deanship of Scientific Research at King Saud University for funding the work through the research group project number RGP-VPP-079.

References

1. Baek M, Hae-Eun Chung J Y, Jung-A L, Tae-Hyun K, Jae-Min O, Won-Jae L, et al. Pharmacokinetics, tissue distribution, and excretion of zinc oxide nanoparticles. I. J. Nanomed 2012; 7: 3081-97.
2. Bihari P, Vippola M, Schultes S, Praetner M, Khandoga AG, Reichel CA et al. Optimized dispersion of nanoparticles for biological in vitro and in vivo studies. Part Fibre Toxicol 2008: 5; 14.1.
3. Breviario F, d'Aniello EM, Golay J, Peri G, Bottazzi B, Bairoch A, et al. Interleukin-1- inducible genes in endothelial cells. Cloning of a new gene related to C-reactive protein and serum amyloid P component. J Biol Chem 1992; 267: 22190 –7.
4. Brigham KL. Role of free radicals in lung injury. Chest 1986; 89: 859–63.
5. Burton K.A. Study of the Conditions and Mechanism of the Diphenylamine Reaction
for the Colorimetric Estimation of Deoxyribonucleic Acid. Biochem J 1956; 62: 315–23.
6. Cho WS, Duffin R, Howie SAM., Scotton CJ, Wallace AH, MacNee W, et al. Progressive severe lung injury by zinc oxide nanoparticles; the role of Zn2+ dissolution inside lysosomes. Particle and Fibre Toxicology 2011; 8: 27- 35.
7. Dubovskiy IM, Martemyanov BB, Vorontsova YL, Rantala MJ, Gryzanova EV, Glupov VV. Effect of bacterial infection on antioxidant activity and lipid peroxidation in the midgut of Gaalleria mellonella L.larva (Lepidoptera, Pyralide). Comparative Biochemistry and Physiology, Part C 2008; 148: 1-5.
8. Feingold KR, Memon RA, Moser AH, Grunfeld C. Paraoxonase activity in the serum and hepatic mRNA levels decrease during the acute phase response. Atherosclerosis 1998; 139: 307–15.
9. Hackenberg S, Zimmermann FZ, Scherzed A, Friehs G, Froelich K, Ginzkey C. Repetitive Exposure to Zinc Oxide Nanoparticles Induces DNA Damage in Human Nasal Mucosa Mini Organ Cultures. Environmental and Molecular Mutagenesis 2011; 52: 582- 9.
10. Han B, Mura M, Andrade C, Okutani D, Lodyga M, Dos Santos CC, et al. TNF-alpha-induced long pentraxin PTX3 expression in human lung epithelial cells via c-Jun Nterminal kinase. J Immunol 2005; 175: 8303–11.
11. Harangi M, Seres I, Varga Z, Emri G, Szilva´ ssy Z, Paragh G, et al. Atorvastatin effect on high-density lipoprotein-associated paraoxonase activity and oxidative DNA damage. Eur J Clin Pharmacol 2004; 60: 685–91.
12. He L, Liu Y, Mustapha A, Lin M. Antifungal activity of zinc oxide nanoparticles against Botrytis cinerea and Penicillium expansum. Microbiol. Res 2011; 166: 207-15.
13. Huang CC, Aronstam RS, Chen DR, Huang YW. Oxidative stress, calcium homeostasis, and altered gene expression in human lung epithelial cells exposed to ZnO nanoparticles. Toxicol in Vitro 2010; 24: 45-55.
14. Hu ML, Chuang CH, Sio HM, Yeh SL. Simple cryoprotection and cell dissociation techniques for application of the comet assay to fresh and frozen rat tissues. Free Radic. Res 2002; 36: 203–209.
15. Jin T, Sun D, Su JY, Zhang H, Sue HJ. Antimicrobial efficacy of zinc oxide quantum dots against Listeria monocytogenes, Salmonella enteritidis, and Escherichia coli. J. Food Sci 2009; 74: M46–M52.
16. Kamata H, Honda S, Maeda S, Chang L, Hirata H, Karin M. Reactive oxygen species promote TNF alpha induced death and sustained JNK activiation by inhibiting MAP kinase phosphatases. Cell 2005; 120: 649–61.
17. Kleinbongard P, Rasaf T, Dejam A, Kerber S, Kelm M. Griess method for nitrite measurement of aqueous and protein containing sample. Meth Enzymol 2002; 359: 158-68.
18. Kroll A, Pillukat MH, Hahn D, Schnekenburger J. Current in vitro methods in nanoparticle risk assessment: limitations and challenges. Eur J Pharm Biopharm 2009; 72: 370–7.
19. Kumon Y, Suehiro T, Ikeda Y, Hashimoto K. Human paraoxonase- 1 gene expression by HepG2 cells is downregulated by interleukin-1β and tumor necrosis factor α, but is upregulated by interleukin-6. Life Sci 2003; 73: 2807–15.
20. Lin W, Xu Y, Huang CC, Ma Y, Shannon KB, Chen DR, et al. Toxicity of nano- and micro-sized ZnO particles in human lung epithelial cells. J Nanopart Res 2009; 11: 25-39.8.
21. Lu S, Duffin R, Poland C, Daly P, Murphy F, Drost E, et al. Efficacy of simple short-term in vitro assays for predicting the potential of metal oxide

nanoparticles to cause pulmonary inflammation. Environ Health Perspect 2009; 117: 241–7.
22. Moron MS, Depierre J, Mannervik B. Levels of glutathione, glutathione reductase and glutathione – S- transferase activities in rat lung and liver. Biochem. Biophys. Acta 1979; 582: 67-78.
23. Nel AE, Madler L, Velegol D, Xia T, Hoek EM., Somasundaran P, et al. Understanding biophysicochemical interactions at the nano-bio interface. Nat Mater 2009; 8: 543–57.
24. Nohynek GJ, Lademann J, Ribaud C, Roberts MS. Grey goo on the skin? Nanotechnology, cosmetic and sunscreen safety. Crit Rev Toxicol 2007; 37: 251–77.
25. Oberdörster G, Maynard A, Donaldson K, Castranova V, Fitzpatrick J, Ausman K, et al Principles for characterizing the potential human health effects from exposure to nanomaterials: elements of a screening strategy. Part Fibre Toxicol 2005; 2: 8-14.
26. Okutani D, Han B, Mura M, Waddell TK, Keshavjee S, Liu M. High-volume ventilation induces pentraxin 3 expression in multiple acute lung injury models in rats. Am J Physiol Lung Cell Mol Physiol 2007; 292: L144–L153.
27. Pereda J, Sabater L, Aparisi L, Escobar J, Sandoval J, Viña J. Interaction between cytokines and oxidative stress in acute pancreatitis. Current medicinal chemistry 2006; 13: 2775-87.
28. Rahman I, Mulier B, Gilmour PS, Watchorn T, Donaldson K, Jeffery PK. Oxidant-mediated lung epithelial cell tolerance: the role of intracellular glutathione and nuclear factor-kB. Biochem Pharmacol 2001; 62: 787–94.
29. Rahman I. The role of oxidative stress in the pathogenesis of COPD: implications for therapy. Treat Respir Med 2005; 4: 175–200.
30. Rahman I. Oxidative stress in pathogenesis of chronic obstructive pulmonary disease: cellular and molecular mechanisms. Cell Biochem Biophys 2005; 43: 167–188.
31. Rasmussen JW, Martinez E, Louka P, Wingett DG. Zinc oxide nanoparticles for selective destruction of tumor cells and potential for drug delivery applications. Expert Opin. Drug Deliv 2010; 7: 1063–77.
32. Roco, M.C. The National Nanotechnology Initiative: Past, Present and Future. 2nd ed; Lyshevski S, Iafrate G, Eds.; Taylor and Francis Press: Boca Raton and London, CRC,; 2007, pp. 1-42.
33. Roy R, Tripathi A, Das M, Dwivedi PD. Cytotoxicity and uptake of zinc oxide nanoparticles leading to enhanced inflammatory cytokines levels in murine macrophages: comparison with bulk zinc oxide. J Biomed Nanotechnol 2011; 7: 110-1.
34. Sayes CM, Reed KL, Warheit DB. Assessing toxicity of fine and nanoparticles: comparing in vitro measurements to in vivo pulmonary toxicity profiles. Toxicol Sci 2007; 97: 163-80.
35. Sharma V, Shukla RK, Saxena N, Parmar D, Das M, Dhawan A. DNA damaging potential of zinc oxide nanoparticles in human epidermal cells. Toxicol Lett 2009: 185, 211-8.
36. Souza DG, Soares AC, Pinho V, Torloni H, Reis LF, Teixeira MM., et al. Increased mortality and inflammation in tumor necrosis factor-stimulated gene-14 transgenic mice after ischemia and reperfusion injury. Am J Pathol 2002; 160: 1755–65.
37. Suenobu N, Shichiri M, Iwashina M, Marumo F, Hirata Y. Natriuretic Peptides and Nitric Oxide Induce Endothelial Apoptosis via a cGMP–Dependent Mechanism. Arterioscler Thromb Vasc Biol 1999; 19: 140-6.
38. Wang B, Feng W, Wang M, Wang T, Gu T, Zhu M, et al. Acute toxicological impact of nano- and submicro-scaled zinc oxide powder on healthy adult mice. J. Nanopart. Res 2007; 10: 263–76.
39. Wang J, Zhou G, Chen C, Yu H, Wang T, Ma Y, et al. Acute toxicity and biodistribution of different sized titanium dioxide particles in mice after oral administration. Toxicol. Lett 2007; 168: 176–85.
40. Wang Y, Oberley LW, Murhhammer DW. Evidence of oxidative stress following the viral infection of two Lepidopteran insect cell lines. Free Rad Biol Med 2001; 31: 1448-55.
41. Uchida K, Shiraishi M, Naito Y, Torii N, Nakamura Y, Osawa T. Activation of stress signaling pathways by the end product of lipid peroxidation. J Biol Chem 1999; 274: 2234–42.
42. Yang H, Liu C, Yang D, Zhang H; Xi Z. Comparative study of cytotoxicity, oxidative stress and genotoxicity induced by four typical nanomaterials: The role of particle size, shape and composition. J Appl Toxicol 2009; 29: 69–78.

1/20/2013